OPTIMAL DESIGN OF MINIATURE PIEZOELECTRIC FANS FOR COOLING LIGHT EMITTING DIODES

Tolga Açıkalın*, **Suresh V Garimella***, **James Petroski**[¶], **and Arvind Raman***

*Purdue University, West Lafayette, Indiana, 47907-2088 USA
sureshg@ecn.purdue.edu

[¶]GELcore, Valley View, OH 44125 USA
Jim.Petroski@gelcore.com

ABSTRACT

Piezoelectric fans have emerged as a viable cooling technology for the thermal management of electronic devices with their low power consumption, minimal noise emission, and small and configurable dimensions. In this work, these fans are investigated for application in the cooling of electronics components and light emitting diodes (LEDs). Different experimental configurations are considered, and the effect of varying the fan amplitude, the distance between the fan and the heat source, the fan length, its frequency offset from resonance, and the fan offset from the center of the heat source are studied to assess the cooling potential of piezoelectric fans. A design-of-experiments (DOE) analysis revealed the fan frequency offset from resonance and the fan amplitude as the critical parameters. Transfer functions are obtained from the DOE analysis for the implementation of these fans in electronics cooling. For the best case, an enhancement in convective heat transfer coefficient exceeding 375% relative to natural convection was observed, resulting in a temperature drop at the heat source of more than 36.4°C.

Keywords: electronics cooling, piezoelectric fans, light emitting diodes, miniature fans, heat sinks

NOMENCLATURE

A	heat source surface area
Gr*	modified Grashof number
%fr	percent frequency
%L	percent length
Nu	Nusselt number
Pr	Prandtl number
q	heat transfer rate
T	temperature
ΔT	temperature differential (drop in heat source temperature with fan relative to natural convective conditions)

Subscript

i	A, B, C, D, or E representing parameters used in the experiment
s	heat source surface
∞	ambient

INTRODUCTION

Natural convection as a preferred means for thermal management (in view of its typical simplicity of implementation) is fast approaching its limits in the face of increasing heat dissipation from electronics in conjunction with consumer demand for smaller devices. Thermal management of LED packages constitutes a good example of such a situation. Although conventional methods for heat removal, such as incorporation of rotational fans are thermally viable, it is the minimized space, power, and noise requirements that point to piezoelectric fans as an alternate method of electronics thermal management.

A piezoelectric fan is fabricated either by bonding a piezoelectric patch (or several patches) to a shim material, or by using the patch itself with no shim attached. Under an alternating voltage, which is applied to the electrodes of the piezoelectric patch, the patch expands and contracts alternately with the same frequency as the input signal. When attached to a shim material, this results in the shim flapping back and forth like a hand-held fan, but at a much higher frequency.

These fans are driven at resonance, meaning that the alternating voltage is applied at the frequency of a resonance mode of the piezoelectric fan. Driving the fan at resonance leads to a high value of the ratio of tip deflection to power consumption. To ensure silent operation, the fans are designed such that their operational mode of resonance (for the intensity of sound generated) is outside the range of frequencies audible to the human ear, *i.e.*, less than 100 Hz for 25 dB.

A number of interesting studies on piezoelectric fans have been reported in the literature. Toda [1,2] experimented with a piezoelectric fan that was fabricated from eight layered sheets of Poly Vinylidene Fluoride (PVF2). This multi-layered bimorph fan was clamped at one end in cantilever fashion and its airflow and cooling capabilities assessed. In a thermal experiment, two of these fans on either side of a power transistor panel of a television receiver resulted in a 17ºC decrease in temperature on the panel surface. Yoo et al. [3] developed several types of piezoelectric fans using

Plumbum (lead) Zirconate Titanate (PZT), one of which resulted in a fan tip deflection of 3.55 cm and an air velocity of 3.1 m/s measured 0.1 cm away from the fan tip. This fan was driven with 110 V and 60 Hz in its first mode of resonance.

Schmidt [4] employed the naphthalene sublimation technique in experiments to determine the local and average transfer coefficients on a vertical surface cooled by two piezoelectric (PVF2) fans resonating out of phase. Changing the distance between the fans and the surface, and the distance from one fan to the other, was found to noticeably change the transfer coefficients for the system.

Flows around the ends of oscillating flexible cantilevers were investigated by Ihara and Watanabe [5]. The discrete vortex method was used to numerically simulate the flow field, which was compared against flow visualizations. Açıkalın et al. [6] developed a closed-form analytical solution to predict the two-dimensional streaming flow from an infinite vibrating beam. This solution was used to develop a computational flow model for a baffled piezoelectric fan vibrating at its 1st mode of resonance in an infinite medium. Experimentally mapped flow patterns were found to closely match those predicted by the model for the baffled fan.

Loh et al. [7] investigated the cooling effects of acoustic streaming from an ultrasonically vibrating beam. A 40ºC temperature drop was observed on a heater which was initially at 98ºC. The beam vibrated at 28 kHz with an amplitude of 25 μm.

Optimization of the structure of piezoelectric fans was investigated by Buermann et al. [8] and Basak et al. [9] who considered fans with two symmetrically placed piezoelectric patches and a piezoelectric patch on only one side, respectively. The studies focused on optimizing the electromechanical coupling factor (EMCF) of these fans.

The feasibility of using piezoelectric fans in small-scale electronics cooling applications was investigated by Açıkalın et al. [10] and Wait et al. [11]. Flow visualization experiments were conducted to gain insight into the flow induced by these fans. The thermal performance of piezoelectric fans was investigated in two different experiments: a custom-built setup was used to quantify the cooling enhancement from a heat-dissipating component due to piezoelectric fans in an enclosure simulating a cellular phone, and a commercially available laptop computer was utilized to demonstrate the viability of using piezoelectric fans for localized cooling. In the first setup, the piezoelectric fans were found to offer enhancements in convective heat transfer coefficients of more than 100% relative to natural convection, while in the latter, a 6ºC to 8ºC temperature drop was observed in the electronic components within the laptop.

In the present study, the potential offered by piezoelectric fans for the thermal management of electronics components and LEDs are assessed. Three different experimental configurations are considered in order to map the effects on the heat transfer from a small heat source of the fan amplitude, the distance between the fan and the heat source, the fan length, its frequency offset from resonance, and the fan offset from the center of the heat source. A design of experiments (DOE) approach is used in the experiments. Transfer functions are obtained from the DOE analysis for the implementation of these fans in electronics cooling.

EXPERIMENTAL SETUP AND PROCEDURES

A typical package was simulated as a constant heat flux source. The heat source was constructed by attaching a kapton thin-film heater to the back of an aluminum plate of dimensions 3.81 cm × 3.81 cm × 0.2 cm. This assembly was imbedded in styrofoam insulation, leaving the heat source flush with the insulation surface (Figure 1), to minimize heat losses from the back and sides of the heat source. The exposed surface of the aluminum plate was painted with Krylon #1602, which has a known emissivity of 0.95 [12].

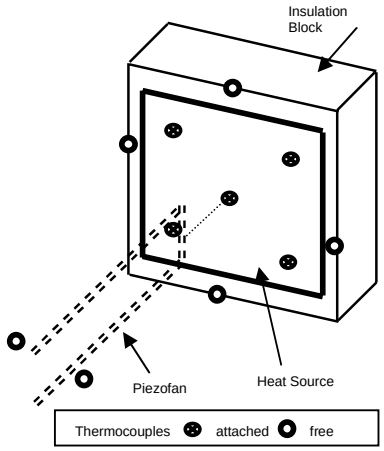

Figure 1. Schematic diagram of the heat source.

Fourteen thermocouples were used to monitor temperatures in the experiments. Of these, five were mounted on the exposed surface of the heat source (to calculate the average surface temperature, as shown in Figure 1), one was sandwiched between the heater and the insulation, and another was attached to the backside of the insulation to provide an estimate of the heat loss. One thermocouple was immersed in a water bath in the enclosure to monitor the ambient air temperature. The remaining six thermocouples are suspended in air, four near the heat source, and two near the fan, as shown in Figure 1. For the finned heat source, three additional thermocouples were inserted into the fin.

A large transparent box (36.6 cm × 36.6 cm × 36.6 cm) was placed around the heat source to isolate the setup from extraneous convection currents in the room as shown in Figure 2. Both the test setup and the piezoelectric fan being studied were mounted on an optical rail, to allow for precise relative positioning.

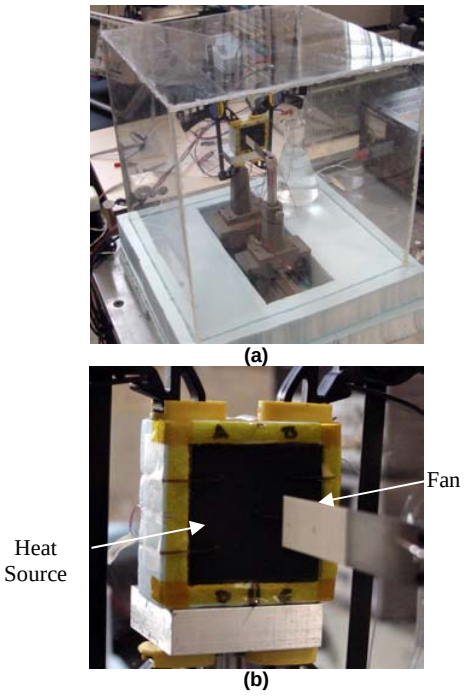

Figure 2. Photographs of a) the experimental setup, and b) detail of the heat source and fan arrangement.

Three different configurations of the piezofan and heat source were studied as shown in Figure 3. In the first two orientations, the position of the fan relative to the heat source was changed, while in the third, a fin was included on the heat source, with the fan position being held the same as in the first case. The fin was 0.15 cm thick and 0.64 cm high, and extended the entire length of the heat source.

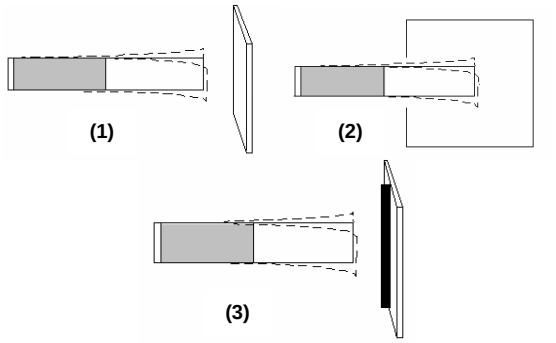

Figure 3. Schematic of different experimental orientations: 1) Fan in front, 2) Fan to the side and 3) Fan in front with fin.

For each of the configurations, the heat transfer coefficient was first measured under natural convective conditions, to provide a baseline. The enhancement of heat transfer upon turning on the piezoelectric fan was then measured and compared to the baseline free convection results.

Five different parameters were varied in these experiments. The frequency offset from the resonance frequency was varied by ± 5%. Three values of input voltage were studied, resulting in three different ratios of tip deflection to fan length under resonance conditions (amplitude ratios) ranging from 10 to 25%. It may be noted that because of this definition of amplitude ratio, the fan amplitude under a frequency offset is lower than its resonance value. The normal distance between the heat source and fan tip at rest (distance to fan tip) as well as the distance along the heat source between fan tip and heat source center were two other parameters, as illustrated in Figure 4. Finally, two piezoelectric fans of different lengths were used to investigate the effect of fan length. This, of course, results in a difference in their resonance frequencies (62 Hz and 103 Hz, respectively for the 7.62 cm and 6.86 cm fans).

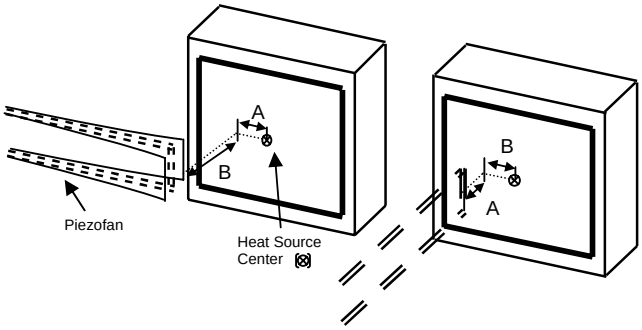

Figure 4. Definitions of two of the parameters studied for different orientations: distance to fan tip (A) and fan offset (B).

The large number of parameters affecting the heat transfer in this experiment suggested the use of a design of experiments (DOE) approach [13]. This approach offers key advantages over typical experimentation methods when several variables are under investigation. The conventional approach is to vary one experimental factor at a time (OFAT) while holding other parameters fixed. This usually does not readily lead to an optimum solution, nor does it allow parameter interactions to be explored. As a result, the goal of optimizing an output, such as heat transfer, may not be realized by the OFAT approach. The DOE process, in contrast, allows for optimal values of the parameters to be predicted, even if actual experiments are not conducted with these values.

Also, a properly constructed DOE can map out transfer functions and response surfaces with fewer experimental runs than by any other methodology. The resolution between the variables is determined by the type of DOE setup that is chosen; the higher the resolution of the DOE, the less is the "confounding" or indistinguishability between combinations of variables. Once a resolution level is chosen, the DOE matrix provides the fewest number of experiments to create the transfer function. Thus a DOE not only provides the best information about a system, but also does so most economically.

RESULTS AND DISCUSSION

Experimental results for Orientation 1 are first discussed in detail, with results for the other two orientations summarized next.

Orientation 1

Results for a sample experiment in this orientation are shown in Figure 5. Measured temperatures for a test with a 7.62 cm long fan operating at resonance with a 25% amplitude ratio (*i.e.*, amplitude to fan length ratio) are shown. The distance to the fan tip is 0.64 cm and there is no fan offset in this test. The total power input to the heat source was 1.6 W, which is consistent with the power dissipation from a high-power LED package of similar size. The power input was corrected for the heat loss through the insulation (which was approximately 0.09 W in natural convection and 0.03 W with the fan operational) in the calculation of heat transfer coefficients. Readings from the fixed thermocouples (see Figure 1) are shown in Figure 5(a), while those from thermocouples suspended in air are shown in Figure 5(b). At t = 0 the heater is turned on and at t ≈ 1500 s, the system reaches a steady state in natural convection. The piezoelectric fan is turned on at t = 2000 s and a new steady state is reached after approximately 500 s. The fan is seen to cause a reduction in the average heat source temperature from approximately 70.6ºC in natural convection to 37.4ºC with the piezofan. The increase in heat transfer coefficient due to the fan causes an increase in the measured air temperatures around the heat source. The heat transfer coefficient in these experiments is defined based on the difference between the average heat source surface temperature and the ambient enclosure temperature.

Similar measurements were obtained for a DOE matrix consisting of a total of 30 experiments for Orientation 1. The lower and upper specification limits (LSL and USL) for the five parameters considered are shown in Table 1.

Table 1. LSL and USL values for Orientation 1.

	LSL	USL
Fan length [cm]	6.86	7.62
Amplitude ratio at resonance [%L]	10	25
Frequency offset [% fr]	-5	5
Plate offset [cm]	0	1.27
Dist to Fan Tip [cm]	0.64	2.54

In Figure 6 the steady-state heat transfer coefficients for three individual experiments from the DOE matrix in Orientation 1 are plotted. The heat transfer coefficients shown in Figure 6 are, of course, effective values, including both convective and radiative effects, and computed as $h = (q_{in}-q_{loss})/[A(T_s-T_\infty)]$, from the measured heat input and surface and ambient temperatures. Also shown in Figure 6 is the effective heat transfer coefficient, computed in the same manner, with the piezofan turned off; a value of 21.62 W/m^{2}K is obtained under these conditions.

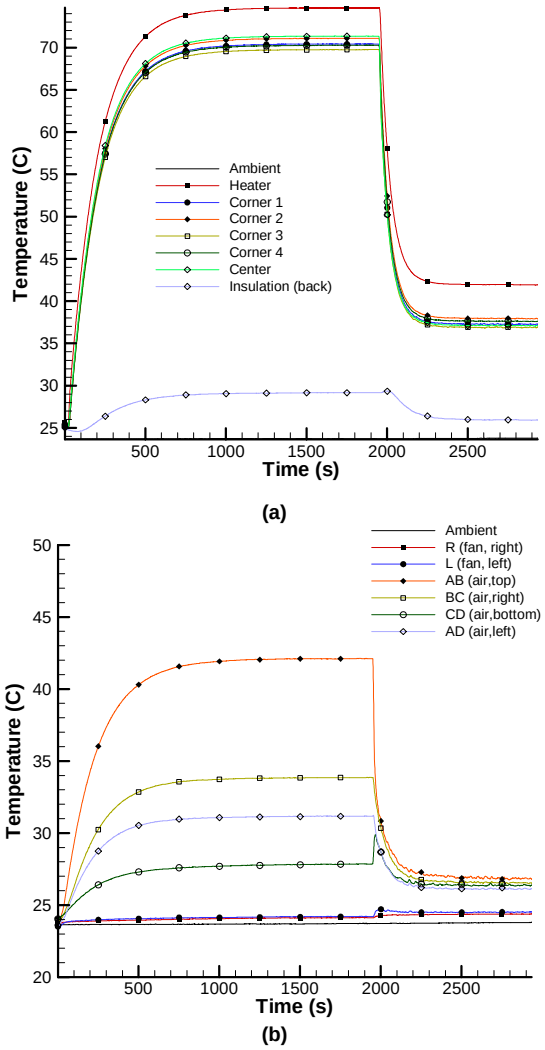

Figure 5. Temperatures from a sample test in Orientation 1: (a) temperatures on the heat source (four corners, center of heat source, between heater and insulation, and back of insulation), and (b) temperatures in air (R and L are on both sides of the fan, while the other four are in air close to the heat source, Figure 1).

The average natural convection coefficient may also be predicted using the following correlation relating the local Nusselt number in laminar natural convection over a vertical flat plate with uniform heat flux [14] to the modified local Grashof number:

$$Nu_x = 0.55\,(Gr_x^* \, Pr)^{0.2}$$

This gives an h value of 11.05 W/m^{2}K. Summed with a predicted radiation component (based on the measured heat source surface temperature) of 7.15 W/m^{2}K, the predicted effective heat transfer coefficient with the fan turned off is 18.2 W/m^{2}K, which compares to the value of 21.62 W/m^{2}K above, obtained directly from the measurements.

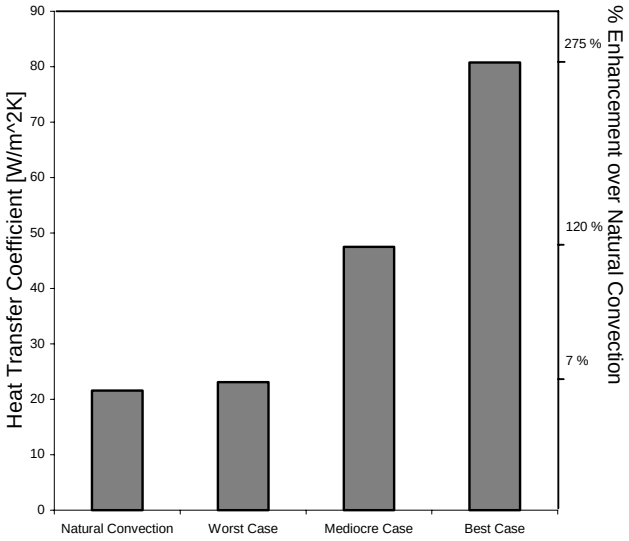

Figure 6. Heat transfer coefficients from three different experiments in Orientation 1, along with the natural convection value.

The average heat transfer coefficients for the 30 experiments in Orientation 1 varied from approximately 23 to 80 W/m^{2}K. Even in the worst case (shown in Figure 6), an approximately 7% enhancement over natural convection was seen. For the best case, an enhancement of greater than 275% over natural convection was achieved.

Results from the DOE analysis are presented in the rest of this paper as a number of surface plots, showing the effects of changes in the governing parameters on the temperature drop achieved on the heat source with the fan relative to the temperatures under natural convection conditions. The frequency offset is revealed to be the most important of the five parameters considered. As the fan is operated farther away from resonance, its amplitude suffers greatly. Since a lower amplitude causes less airflow, the cooling capacity of the fan decreases correspondingly. Figure 7 shows the influence of frequency offset and fan distance on the temperature differential achieved at the heat source. A frequency offset of 5% (3.1 Hz) is seen to decrease the cooling capacity of the fan by 10ºC (under optimal values for the remaining four factors). Moving the fan further away from the heat source resulted in an expected drop in performance: the extreme positions of the fan considered caused a difference of approximately 10ºC in the temperature of the heat source. It may be noted that the optimum value of fan-to-tip distance resides outside of the DOE tests, and heat transfer from the surface would increase as the distance is reduced below 0.64 cm; this is consistent with the observations in [4]. As for the other parameters, Figure 8 shows that halving the tip deflection of the fan (from 25% to 12.5% of fan length) reduces the temperature of the heat source by 16.4ºC. Although displacing the fan to one side (increasing the offset) decreases the cooling achieved, this effect is much smaller than the other three factors discussed.

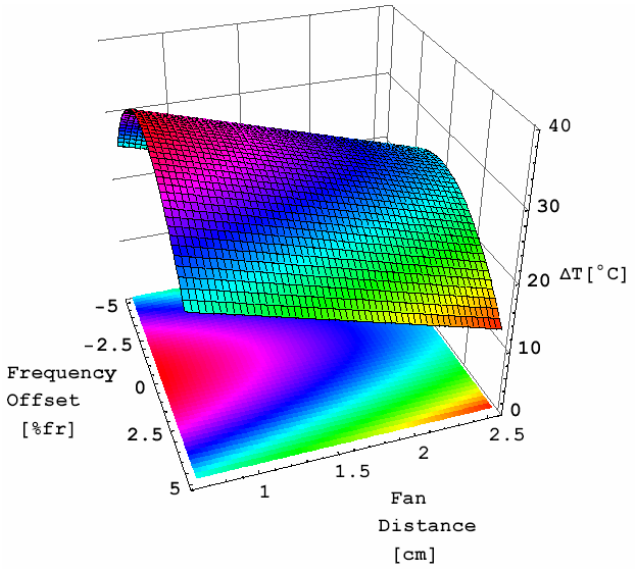

Figure 7. Heat source temperature differential for Orientation 1, for varying frequency offset and fan-heat source distance (for a 7.62 cm fan with an amplitude of 25 % and no fan offset). In this and all similar shadow 3D plots in this paper, a projection of the surface on a horizontal plane is also included as a visual aid.

In the context of the experiments performed here, the shorter fan always performs better than the longer fan. The two fans of different length have quite different resonance frequencies (62 Hz and 103 Hz, respectively for the 7.62 cm and 6.86 cm fans). This difference in resonance frequencies, in conjunction with the amplitudes of vibration being quite similar in the two cases, results in higher fluid velocities in the case of the shorter fan. The temperature differential is found to be 10% to 20% greater when the shorter fan is used; the temperature differential is affected more strongly at the lower fan amplitudes.

The transfer function obtained from the DOE analysis for the temperature drop on the heat source in Orientation 1 is given below, where R_i are the standardized parameters in the order shown in Table 1 (R_A represents fan length, etc.). In this context, "standardized" means –1 for the lower specification limit (LSL), 1 for the high limit (USL), and 0 for the mean value. This transfer function predicts the experimental observations with a correlation coefficient R^2 of 0.98.

$$\Delta T = -3.26 \cdot R_A + 6.60 \cdot R_B - 0.87 \cdot R_C - 0.21 \cdot R_D - 2.77 \cdot R_E - 0.91 \cdot R_B \cdot R_E - 7.91 \cdot R_C^2 - 0.44 \cdot R_C \cdot R_D + 0.48 \cdot R_D \cdot R_E + 26.58$$

The transfer function for the heat transfer coefficient was also computed but is not included here.

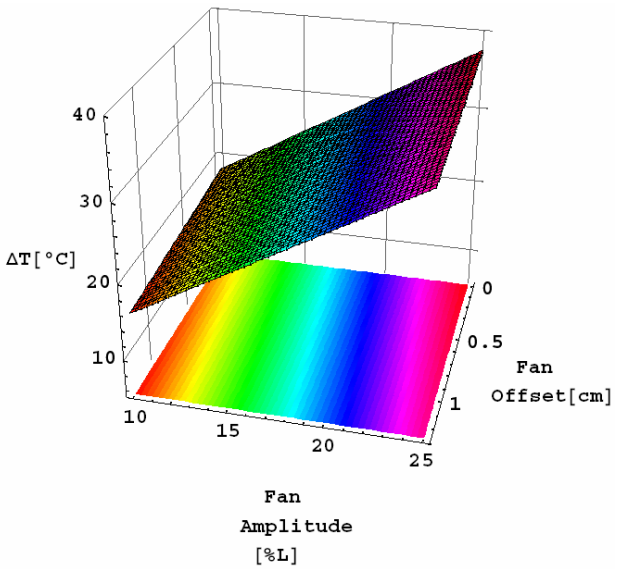

Figure 8. Heat source temperature differential for Orientation 1, for varying fan offset and fan amplitude (for a 7.62 cm fan with a fan distance of 0.64 cm and no frequency offset).

In view of the predictions from the DOE results, an additional experiment was conducted at the "best predicted" point (with the five parameter values set at the optimal values pointed out by the DOE) and an enhancement of more than 375% over natural convection was achieved for this orientation, matching the transfer function model. This best performance is obtained at a fan length of 6.86 cm, amplitude ratio of 25%, fan-to-heat source distance of 0.64 cm and without any frequency or fan offset. Under these conditions a temperature differential of 36.4ºC and an average heat transfer coefficient of 100.8 W/m^2K were achieved.

Orientation 2

In Orientation 2, the piezofan was placed parallel to the heat source (Figure 3). As shown in Table 2, the only parameters that were given different LSL and USL values when compared to Orientation 1 were the fan offset and distance between the heat source and fan. Also, the distance between the heat source and fan tip in this orientation is referenced from the deflected fan position when the tip is closest to the heat source (Distance B in Figure 4).

Table 2. LSL and USL values for Orientation 2.

	LSL	USL
Fan length [cm]	6.86	7.62
Amplitude ratio at resonance [%L]	10	25
Frequency offset [% fr]	-5	5
Plate offset [cm]	-1.27	1.27
Dist to Fan Tip [cm]	0.64	1.9

The results of the DOE analysis for this orientation are shown in Figure 9 and Figure 10. It is again clear from these results that the frequency offset is the most important determinant of heat transfer. As the fan is operated farther off-resonance, its amplitude decreases as does its cooling capability. Figure 9 shows a decrease in cooling capacity of more than 15ºC for a frequency offset of 5%. As in Orientation 1, moving the fan further away from the heat source results in a performance drop. In contrast to Orientation 1, however, the fan offset plays a more significant role in Orientation 2, and causes a drop in temperature differential on the heat source of approximately 12ºC, when compared to the original fan position.

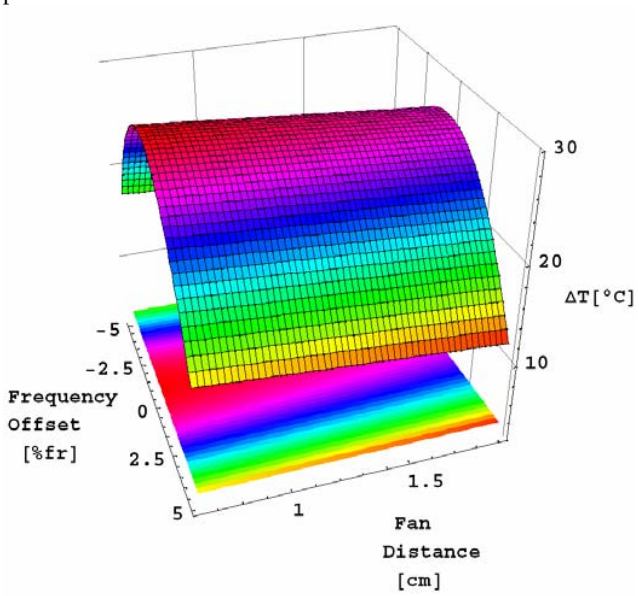

Figure 9. Heat source temperature differential for Orientation 2, for varying frequency and fan-heat source distance (for a 7.62 cm fan with an amplitude of 25% and no fan offset).

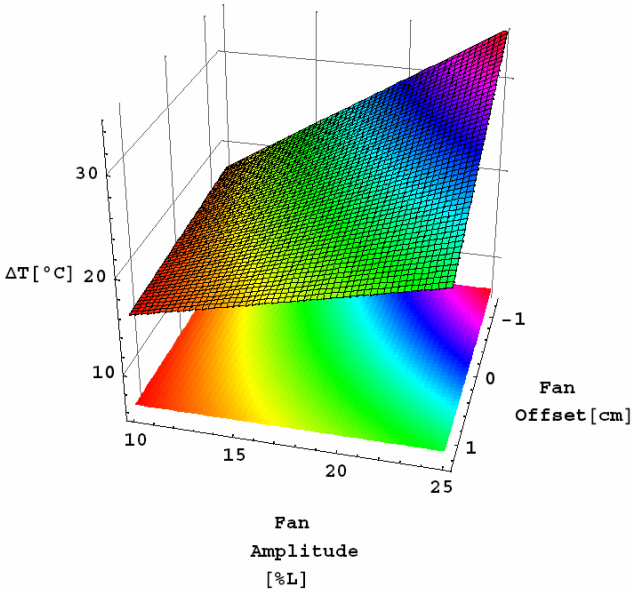

Figure 10. Heat source temperature differential for Orientation 2, for varying fan amplitude and fan offset (for a 7.62 cm fan with a fan distance of 0.64 cm and no frequency offset).

The transfer function obtained from the DOE analysis for the temperature drop on the heat source in Orientation 2 is given below:

$$\Delta T = -2.07 \cdot R_A + 4.87 \cdot R_B - 1.06 \cdot R_C - 2.66 \cdot R_D - 0.88 \cdot R_E - 1.69 \cdot R_B \cdot R_D - 8.25 \cdot R_C^2 - 0.62 \cdot R_C \cdot R_D + 23.79$$

Orientation 3

This orientation is identical to Orientation 1, with the difference that instead of a flat heat source, a finned version is used, as explained earlier (Figure 3). Because of the increased surface area, 1.8 W of power input is required in this case to maintain the heat source surface temperature at 72ºC**.** Table 3 shows the LSL and USL values for the parameters studied in this orientation. One common parameter between all three orientations is the fan to heat source distance, which is 0.64 cm. It is noted that in Orientation 3, this distance is measured not from the plane of the heat source but instead from the tip of the fin, making the total distance from the heat source plane 1.27 cm.

Table 3. LSL and USL values for Orientation 3.

	LSL	USL
Fan length [cm]	6.86	7.62
Amplitude ratio at resonance [%L]	10	25
Frequency offset [% fr]	-5	5
Plate offset [cm]	0	0
Dist to Fan Tip [cm]	0.64	1.9

As seen from Figure 11 and 12, Orientation 3 has similar trends as Orientation 1. In Orientation 3, the temperature differentials are slightly lower than those in Orientation 1; however, Orientation 3 has 13% greater heat dissipation.

Due to the presence of the fin, the fan offset parameter was not investigated and the fan was always centered with respect to the finned heat source. Thus the transfer function derived does not contain any fan offset terms (R_D):

$$\Delta T = -3.33 \cdot R_A + 7.33 \cdot R_B - 0.95 \cdot R_C - 2.11 \cdot R_E - 0.99 \cdot R_A \cdot R_B - 0.67 \cdot R_A \cdot R_C - 0.94 \cdot R_B \cdot R_E + 7.91 \cdot R_C^2 + 25.89$$

Comparison of Orientations

In Figure 13, DOE results from Figures 7, 9 and 11 are plotted together to facilitate comparison. From this figure it is seen that the temperature differential is highest for Orientation 1 and lowest for Orientation 2. In all three orientations, the frequency dependence of the temperature differential is similar. However the effect of fan distance on the temperature differentials is quite different: Orientations 1 and 3 are more strongly dependent (have a higher slope) on the fan distance than Orientation 2.

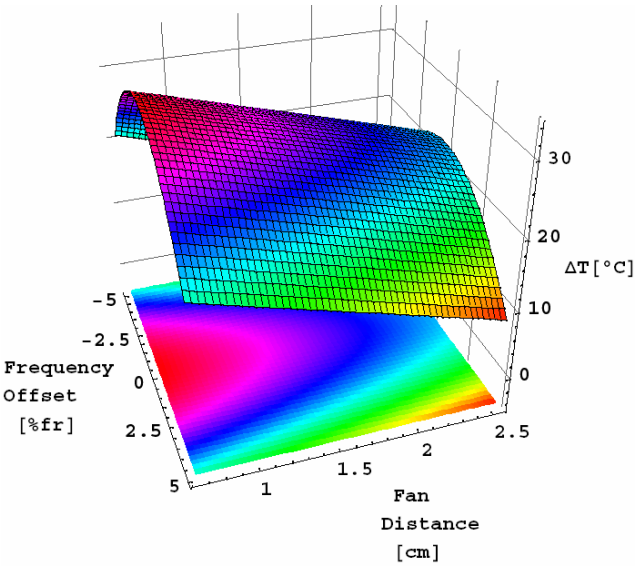

Figure 11. Heat source temperature differential for Orientation 3, for varying frequency and fan-heat source distance (for a 7.62 cm fan with an amplitude of 25%).

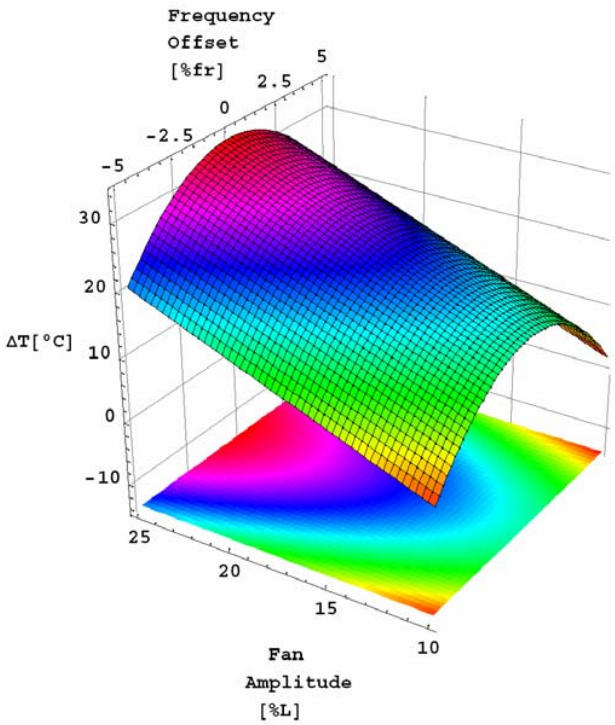

Figure 12. Heat source temperature differential for Orientation 3, for varying frequency and fan amplitude (for a 7.62 cm fan with a fan distance of 0.64 cm).

Although Orientation 3 has a lower temperature differential than Orientation 1, it has higher average heat transfer coefficients. This is illustrated for three comparable experiments for the two orientations in Figure 14. The use of a heat transfer coefficient accounts for the difference in heat inputs in the two orientations. Plotted in this manner, it is clear that inclusion of the fin enhanced the heat transfer significantly. This increase in heat transfer coefficient is in spite of an increase in the heat source to fan distance.

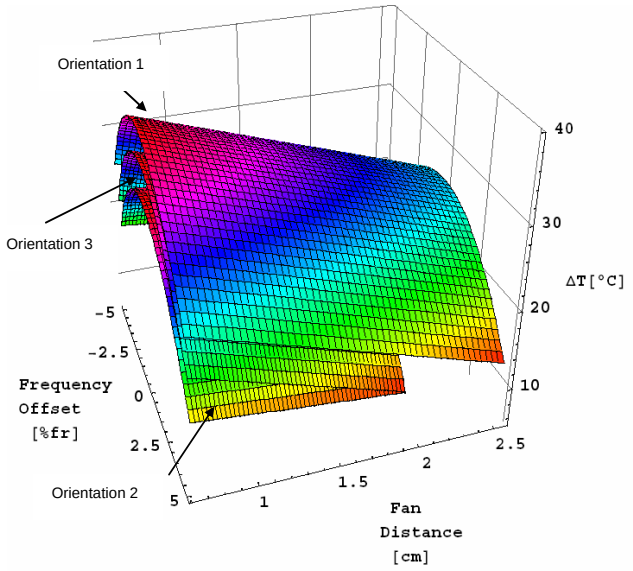

Figure 13. Comparison of DOE results from Figures 7, 9, and 11.

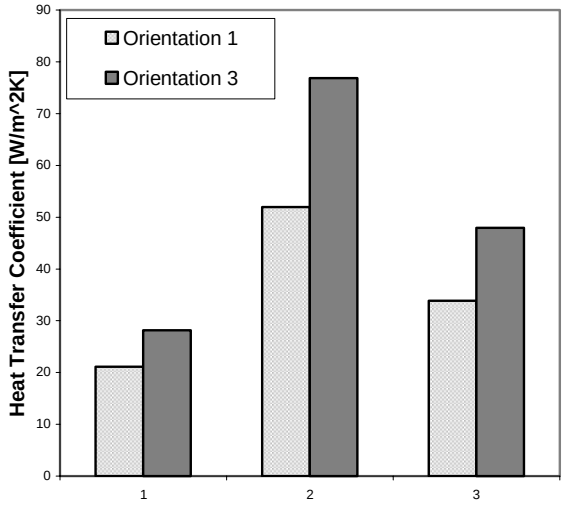

Figure 14. Comparison of individual experiments from Orientations 1 and 3, illustrating the effect of inclusion of the fin.

In Figure 15, temperature differentials achieved on the heat source in Orientations 1 and 2 are compared for different fan amplitude and fan offset. Since there is no fan offset in Orientation 3, it is not included in this figure. Also, the fan offset in Orientation 1 is in only one (*i.e.*, positive) direction, since this parameter is symmetric with respect to the centerline of the heat source in this orientation. The figure shows that the dependence of the temperature differential in Orientation 1 on fan amplitude is stronger than in Orientation 2. On the other hand, the dependence on the fan offset is much greater in Orientation 2.

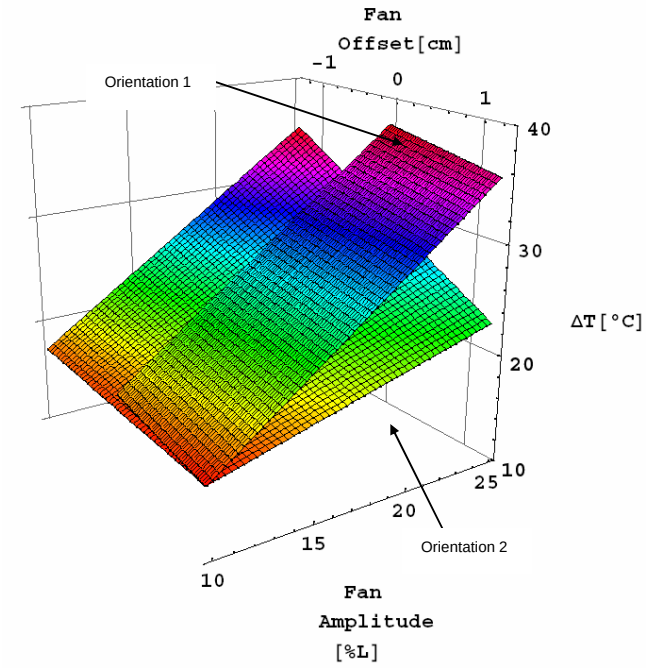

Figure 15. Comparison of DOE results from Figures 8 and 10.

SUMMARY AND CONCLUSIONS

Piezoelectric fans have been shown to be a viable solution for the thermal management of electronics component and LED packages. The fans reduced the temperature of the heat source by as much as 37.4ºC, from values in natural convection of 70.6ºC. Transfer functions are presented for three different practical orientations of the fan and heat source. These transfer functions can be used in combination in the implementation of piezoelectric fans in complex heat sinks and LED packages.

Acknowledgments

Financial support for this work from GELcore is acknowledged.

REFERENCES

[1] M. Toda, "Voltage-induced Large Amplitude Bending Device-PVF_2 Bimorph-Its Properties and Applications," Ferroelectrics, vol. 32, pp. 127-133, 1981.

[2] M. Toda, "Theory of Air Flow Generation by a Resonant Type PVF_2 Bimorph Cantilever Vibrator," Ferroelectrics, vol. 22, pp. 911-918, 1979.

[3] J. H. Yoo, J. I. Hong, and W. Cao, "Piezoelectric Ceramic Bimorph Coupled to Thin Metal Plate as Cooling Fan for Electronic Devices," Sensor Actuators A Phys, vol. 79, pp. 8-12, 2000.

[4] R. R. Schmidt, "Local and Average Transfer Coefficients on a Vertical Surface Due to Convection from a Piezoelectric Fan," InterSociety Conference on Thermal Phenomena, pp. 41- 49, 1994.

[5] A. Ihara, and H. Watanabe, "On the Flow around Flexible Plates, Oscillating With Large Amplitude," J. Fluid. Struct., vol. 8, pp. 601-619, 1994.

[6] T. Açıkalın, A.Raman, and S.V. Garimella "Two-Dimensional Streaming Flows Induced by Resonating, Thin Beams," J. Acoust. Soc. Am., Vol. 114, pp. 1785–1795, 2003.

[7] B. G. Loh, S. Hyun, P. I. Ro, and C. Kleinstreuer, "Acoustic Streaming Induced by Ultrasonic Flexural Vibrations and Associated Enhancement of Convective Heat Transfer," J. Acoust. Soc. Am., vol. 111, 875-883, 2002.
[8] P. Buermann, A. Raman and S. V. Garimella, "Dynamics and Topology Optimization of Piezoelectric Fans," IEEE Transactions on Components and Packaging Technologies, Vol. 25, pp. 113-121, 2002.
[9] S. Basak, A. Raman and S. V. Garimella, "Dynamic Response Optimization of Asymmetrically Configured Piezoelectric Fans," ASME 19th Biennial Conference on Mechanical Vibration and Noise, Chicago, Illinois, September 2-6, 2003.
[10] T. Açıkalın, S. Wait, S. V. Garimella and A. Raman, "Experimental Investigation of the Thermal Performance of Piezoelectric Fans," Heat Transfer Engineering, Vol. 25, pp. 4-14, 2004.
[11] S. Wait, T. Açıkalın, S. V. Garimella and A. Raman, "Piezoelectric Fans for the Thermal Management of Electronics," Sixth ISHMT/ASME Heat and Mass Transfer Conference, Kalpakkam, India, January 5-7, 2004
[12] NASA Jet Propulsion Laboratory Web Site, URL: http://masterweb.jpl.nasa.gov/reference/paints.htm
[13] S.R. Schmidt, and R. G. Launsby, *Understanding Industrial Designed Experiments*, 4th edition, Colorado Springs, CO, 2003
[14] G.C. Vliet, and D.C. Ross, "Turbulent Natural Convection on Upward and Downward Facing Inclined Constant Heat Flux Surfaces," J. Heat Trans., vol. 97, pp. 549-555, 1975.